

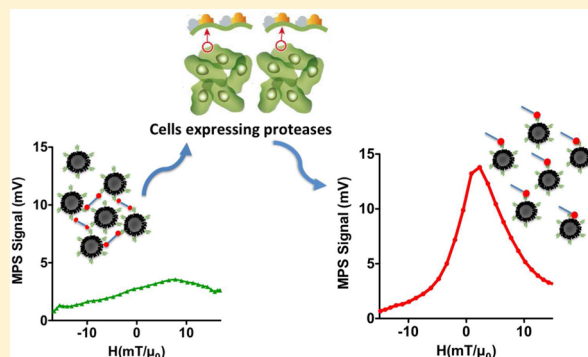
# Detection of Cancer-Specific Proteases Using Magnetic Relaxation of Peptide-Conjugated Nanoparticles in Biological Environment

Sonu Gandhi,<sup>†</sup> Hamed Arami,<sup>†</sup> and Kannan M. Krishnan<sup>\*,†</sup>

<sup>†</sup>Materials Science & Engineering Department, University of Washington, Seattle, Washington 98195–2120 United States

## S Supporting Information

**ABSTRACT:** Protease expression is closely linked to malignant phenotypes of different solid tumors; as such, their detection is promising for diagnosis and treatment of cancers, Alzheimer's, and vascular diseases. Here, we describe a new method for detecting proteases by sensitively monitoring the magnetic relaxation of monodisperse iron oxide nanoparticles (IONPs) using magnetic particle spectrometer (MPS). In this assay, tailored peptides functioning as activatable nanosensors link magnetic nanoparticles and possess selective sites that are recognizable and cleavable by specific proteases. When these linker peptides, labeled with biotin at N- and C-terminals, are added to the neutravidin functionalized IONPs, nanoparticles aggregate, resulting in well-defined changes in the MPS signal. However, as designed, in the presence of proteases these peptides are cleaved at predetermined sites, redispersing IONPs, and returning the MPS signal(s) close to its preaggregation state. These changes observed in all aspects of the MPS signal (peak intensity, its position as a function of field amplitude, and full width at half-maximum—when combined, these three also eliminate false positives), help to detect specific proteases, relying only on the magnetic relaxation characteristics of the functionalized nanoparticles. We demonstrate the general utility of this assay by detecting one each from the two general classes of proteases: trypsin (digestive serine protease, involved in various cancers, promoting proliferation, invasion, and metastasis) and matrix metalloproteinase (MMP-2, observed through metastasis and tumor angiogenesis). This MPS based protease-assay is rapid, reproducible, and highly sensitive and can form the basis of a feasible, high-throughput method for detection of various other proteases.



**KEYWORDS:** Iron oxide nanoparticle, magnetic particle spectroscopy, protease assay, peptide, matrix metalloproteinase

Protease-based therapies offer efficient and effective tools for the development of sensitive assays to investigate the role of protease in physiological processes such as blood clotting, digestion, and disease progression.<sup>1–3</sup> Proteolytic enzymes are important in the breakdown of long polypeptide chains of proteins into shorter peptide fragments and eventually into amino acids.<sup>4</sup> Overexpression of proteases (e.g., matrix metalloproteinase (MMPs), trypsin, caspases, and thrombin) are linked to various pathological phenomena such as cancers, neurodegenerative disorders, cardiovascular diseases, and gastric ulcer.<sup>5–7</sup> Therefore, developing sensitive techniques for detecting proteases in various biological environments is important for further understanding their function and developing antiprotease therapeutics.<sup>8</sup>

In this report, we describe a new magnetic relaxation based assay and illustrate its utility by focusing on two major proteases: trypsin and MMPs. Trypsin is a serine protease and an important enzyme in digestive system. Trypsin reliably cleaves proteins or peptides at the carboxyl terminal of lysine and arginine. Unregulated trypsin secretion results in pancreatic diseases such as maldigestion disorder, chronic pancreatitis, cancer proliferation, and metastasis.<sup>8–11</sup> Therefore, it is important to develop convenient protease assays for its

detection in tissue culture medium and tissue extracts for therapeutic purposes. Similarly, among several MMPs proteases, MMP-2 is known to be involved in the degradation of extracellular matrix proteins that play a major role in normal physiological processes, such as embryonic development, and tissue remodeling, as well as in disease progression, such as in arthritis, cancer invasion, and metastasis.<sup>12,13</sup> MMP-2 also has a specific recognition site at the leucine residue that can be used for cleavage by MMP protease.<sup>14</sup>

Developing new methods for detecting and screening protease inhibitors is also important in diagnosis of diseases (e.g., cancers and gastric ulcers) based on protease therapy. Conventional methods used for the detection of these enzymes involve gel electrophoresis, enzyme-linked immunosorbent assays (ELISA), and high-performance liquid chromatography (HPLC).<sup>15–18</sup> For higher sensitivity and accuracy, protease detection assays are mostly based on the use of radioisotopes; however, the major disadvantages of using radioactive compounds are their short half-lives and environmental and

**Received:** February 29, 2016

**Revised:** May 18, 2016

**Published:** May 24, 2016

personnel safety concerns.<sup>19–22</sup> In addition, over the past decade, numerous fluorescence-based methods have been developed for protease detection.<sup>23–25</sup> The use of fluorogenic compounds for detecting proteases is also challenging, due to quenching mechanism (liberation of a fluorescent product from a fluorogenic reactant measured by fluorometer), which results in limited efficacy for each substrate.<sup>26–29</sup> Hence, although existing techniques are consistently used for qualitative and quantitative detection, to overcome several drawbacks such as the need for sophisticated instrumentation and the necessity of using trained personnel, and radioactive or fluorescent tags, requires the development of an alternative facile and reliable method such as the one reported here.

Superparamagnetic iron oxide nanoparticles are biocompatible materials<sup>30</sup> with extensive diagnostic and therapeutic applications,<sup>31</sup> including biomedical imaging, drug delivery, and gene therapy.<sup>31–34</sup> Further, the magnetic properties and magnetic relaxation dynamics of IONPs can also be effectively used for detection of various proteases. Zhao et al. demonstrated a magnetic resonance imaging (MRI)-based technique for detecting trypsin, renin, and MMP protease activity using superparamagnetic nanoparticles as magnetic relaxation switches (MRS).<sup>28</sup> They determined the protease activity, *indirectly*, by measuring changes in spin relaxation time ( $T_2$ ) of water molecules caused by these nanoparticles in a MRI system. Here, we demonstrate an alternative, simple, inexpensive, quick, and reproducible, IONPs-based protease assay by using magnetic particle spectrometry (MPS). MPS provides a highly sensitive, rapid, and quantitative measurement of nanoparticle magnetization and relaxation response under ac excitation and was developed in conjunction with an emerging biomedical imaging modality called magnetic particle imaging (MPI).<sup>35–40</sup> In MPS, an alternating magnetic field is applied to magnetic nanoparticles in solution, and then the field-dependent derivative of the magnetization,  $dm(H)/dH$ , is measured.<sup>41</sup> The MPS signal—peak height, half-width, and position—is highly dependent on the relaxation mechanism (i.e., Néel, Brownian, or hysteretic reversal) of the nanoparticles, which in turn, for a fixed applied frequency or measurement time, is a strong function of their size, interparticle interactions, surface functionalization, and the surrounding environment.<sup>42,43</sup>

In this report, we utilize the magnetic relaxation dynamics of size-optimized, and specifically surface functionalized, nanoparticles in a MPS system to develop a novel method for detection of protease (Figure 1) and demonstrate the general utility of this technique using two representative cancer specific proteases (i.e., trypsin and MMP-2). First, we synthesized highly monodisperse 22 nm superparamagnetic IONPs and functionalized them with poly(maleic anhydride-*alt*-1-octadecene) (PMAO) polymer to introduce carboxyl groups on the surface of nanoparticles. These carboxyl groups were used to conjugate the amino group ( $\text{NH}_2$ ) of neutravidin using carbodiimide chemistry (Figure 2A). Then, we used specifically designed linker peptides that act as neutravidin cross-linking molecules, to aggregate the neutravidin-coated nanoparticles. In addition, these linker peptides were chosen such that they are selectively recognized and cleaved by the specific proteases (trypsin or MMP-2), resulting in the redispersion of the aggregated nanoparticles. The state of the magnetic nanoparticles, aggregated or dispersed, can be accurately measured by MPS, due to specific and reproducible changes in their magnetic relaxation characteristics (Figure 1). Thus, by

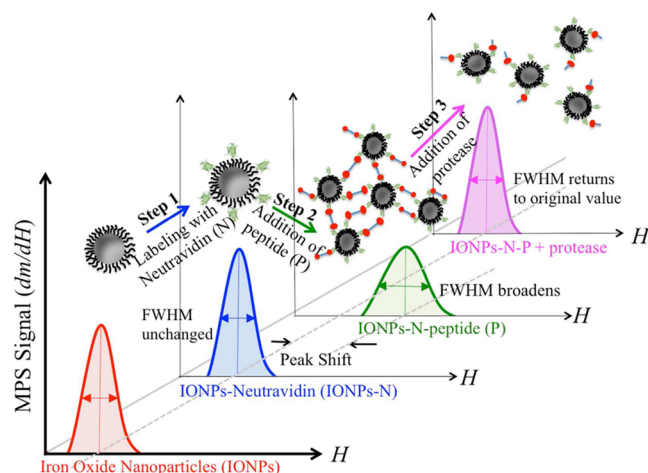


**Figure 1.** Mechanism of magnetic protease sensing based magnetic particle spectroscopy,  $dm(H)/dH$ . The magnetic response (MPS peak intensity, position, and fwhm) of the IONPs do not change after their functionalization with neutravidin (IONPs-N, step 1). Addition of specifically designed peptides (P) (GK-8 and GK-9) to the IONPs-N complex, in step 2, results in aggregation of nanoparticles due to the interaction of neutravidin and biotin. This phenomenon decreased the MPS signal intensity, increases its fwhm, and shifts the peak position. Proteases such as trypsin and MMP-2, added to these aggregates (IONPs-N-P), cleaved the linker peptides between the nanoparticles, and redispersed them (step 3). The MPS signal (intensity, position, and fwhm) of the redispersed nanoparticles is similar to their preaggregation state. The sensitivity of the multiple magnetic relaxation signals of the samples, to the cleaving of the linker peptide by the specific protease, forms the basis of their detection in different biological environment.

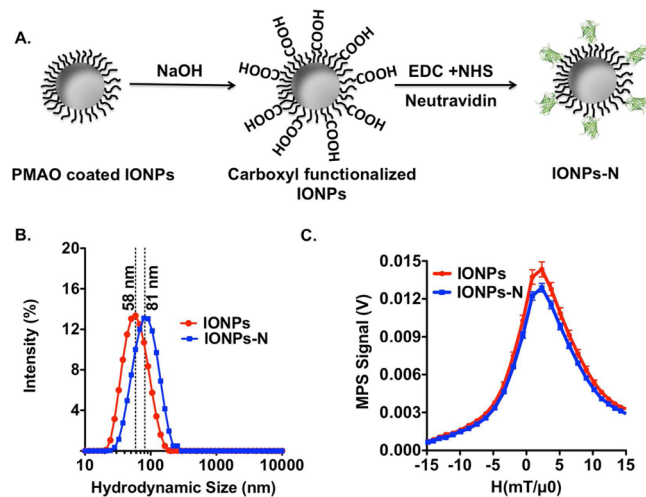


**Figure 2.** (A) Synthesis, phase transfer, and functionalization of the iron oxide nanoparticles (IONPs), followed by their coating with neutravidin (N); (B) DLS plots of IONPs and IONPs-N, showing hydrodynamic diameters of  $\sim 58$  nm with polydispersity index (PDI: 0.156) and  $\sim 81$  nm (PDI: 0.168), respectively; (C) MPS spectra of the nanoparticles, showing that  $dm/dH$  signal intensity (peak height) and fwhm, remained unchanged before and after neutravidin conjugation.

measuring the magnetic relaxation of the nanoparticles in a MPS, the protease responsible for the cleavage of the selected peptide can be detected; a potentially useful assay for various biomedical purposes such as cancer and gastric ulcer diagnosis.

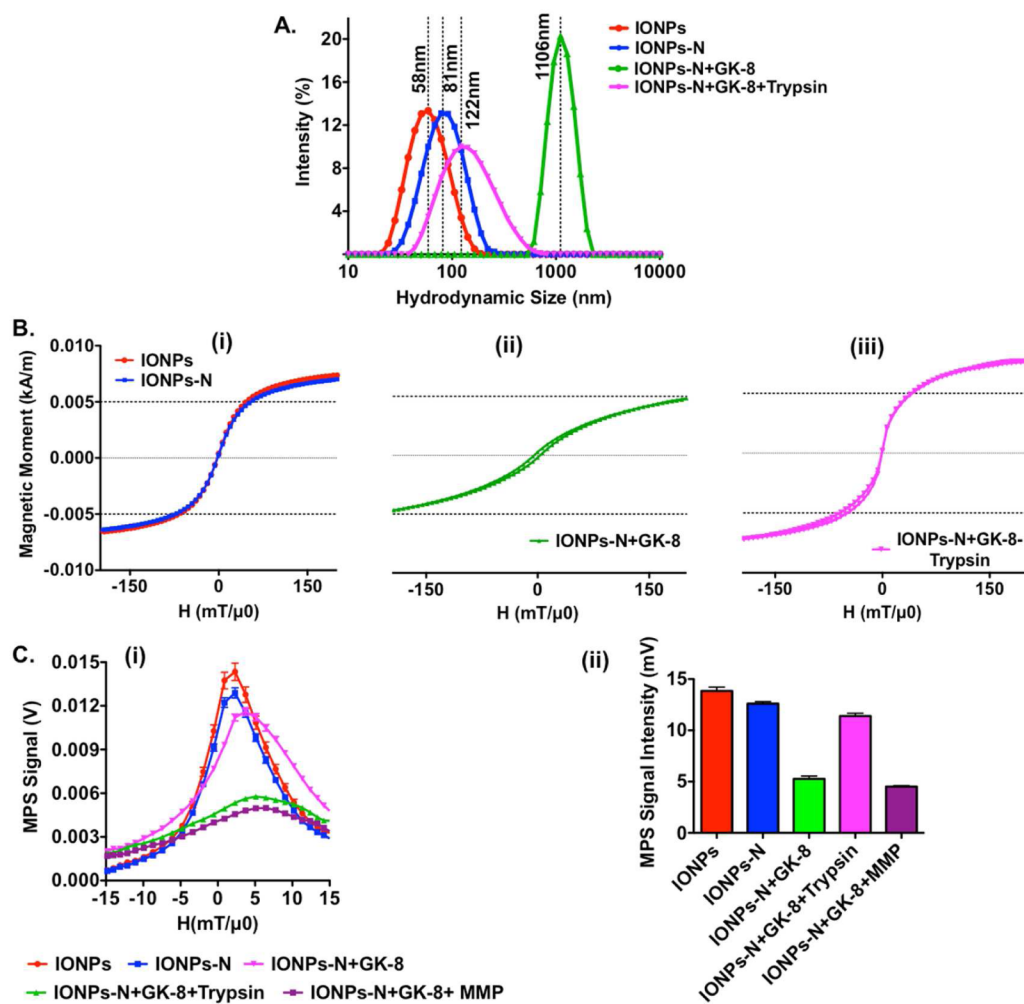


**Figure 3.** Magnetic assay for detection of trypsin using a trypsin-cleavable linker peptide (GK-8). Addition of this peptide to IONPs-N, resulted in aggregation of the nanoparticles. However, these aggregated nanoparticles get redispersed after addition of trypsin. (A) DLS measurements show the hydrodynamic diameters of the nanoparticles at different stages, before and after loading of GK-8 peptide to neutravidin coated nanoparticles and after addition of trypsin. Aggregated nanoparticles (IONPs-N-GK-8) had significantly larger hydrodynamic size, which decreased significantly upon addition of trypsin; (B) VSM plots of IONPs, IONPs-N, IONPs-N+GK-8, and IONPs-N+GK-8+Trypsin show a decrease in magnetization slope of the nanoparticles at near zero field regions, and formation of open magnetization loops when the nanoparticles were aggregated in the presence of GK-8 peptide (IONPs-N-GK-8). The magnetization slope increased, and the magnetization open loop disappeared (showing superparamagnetic behavior) after redispersion of the nanoparticles due to presence of trypsin (IONPs-N-GK-8-Trypsin); (C) MPS ( $dm/dH$ ) spectra show sharper MPS peaks of the nanoparticles, both before the addition of the peptide and after addition of trypsin. In addition, fwhm of the redispersed nanoparticles (IONPs-N-GK-8-Trypsin) decreased to  $\sim 14 \text{ mT}\mu_0^{-1}$ , and its peak intensity increased ( $\sim 2.4$  fold) after addition of trypsin protease to the aggregated complex.

Design of specific peptides for such magnetic assays is routine and, unlike other methods mentioned earlier, precludes the need for unsafe radioactive isotopes or the use of fluorogenic substrates with quenching constraints; further, it also offers the possibility of a “mix and detect” approach, as demonstrated, for quick detection of proteases in biological environments by MPS (e.g., cell culture media, tissue extracts, blood, and urine). Finally, MPS has a simple design that can be easily modified for multiplex magnetic-based assays by measuring the signals from a large number of samples simultaneously.

**Characterization of Iron Oxide Nanoparticles.** IONPs were prepared by thermal decomposition of iron oleate precursor in the presence of oleic acid surfactant.<sup>44</sup> TEM analyses (Figure S1. A (i and ii)) showed that the synthesized nanoparticles were highly monodispersed with median core size of  $22 \pm 1.94 \text{ nm}$ , in agreement with their size calculated from their magnetization curves (Figure S1. B).<sup>45</sup> Such size

monodispersity is crucial for the development of this protease assay, since the magnetic response of the IONPs is highly dependent on their size and size-distribution.<sup>42</sup> IONPs were coated with PMAO polymer using the strong hydrophobic interactions between oleic acid molecules on their surface and octadecene aliphatic chains of PMAO.<sup>37</sup> 0.1 M sodium hydroxide solution was used for hydrolysis of maleic anhydride groups of PMAO and generation of free carboxyl groups ( $-\text{COOH}$ ) on the surface of the IONPs;<sup>46,47</sup> these carboxyl groups were then activated by standard carbodiimide chemistry using EDC and NHS and then, neutravidin was covalently conjugated to the activated IONPs (Figure 2A). The carboxyl groups were introduced to provide a chemically active functional group for the interaction between neutravidin and IONPs. Also, their modest negative charge (zeta potential  $\sim 7 \text{ mV}$ ) helps to increase the dispersion of IONPs in aqueous



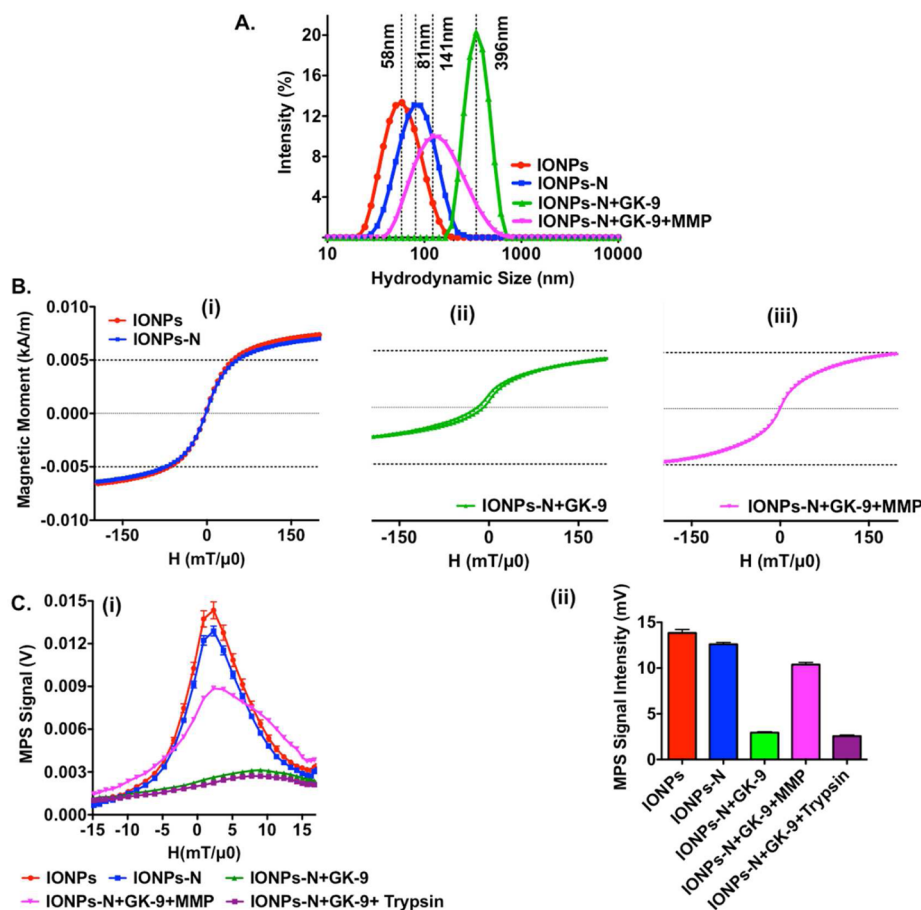


**Figure 4.** MMP protease detection assay, using nanoparticles aggregated with MMP-2 peptide (GK-9). (A) DLS measurements clearly confirm our VSM and MPS observations, regarding the aggregation and redispersion of the nanoparticles; (B) VSM plots of IONPs, IONPs-N, IONPs-N+GK-9, and IONPs-N+GK-9+MMP. The aggregation of the nanoparticles after addition of the GK-9 peptide causes an open loop in  $m-H$  measurement of the nanoparticles (IONPs-N-GK-9, part B (ii)), showing their slightly ferromagnetic characteristic. However, nanoparticles show a closed-loop superparamagnetic behavior both before aggregation and when they get redispersed due to presence of MMP-2 protease; (C) MPS measurement of the aggregated nanoparticles shows lower signal intensity (3 mV) and larger fwhm values ( $30 \text{ mT}\mu_0^{-1}$ ). Signal intensity increased to 8 mV, and fwhm was decreased to  $12 \text{ mT}\mu_0^{-1}$  after redispersion of the nanoparticles, in the presence of MMP protease. These results are similar to the trypsin detection observations shown in Figure 3.

solutions due to the electrostatic repulsion between individual particles.

**Conjugation of Neutravidin to Iron Oxide Nanoparticles.** Neutravidin has a high binding affinity to biotin ligands (dissociation constant,  $K_d = 10^{-15} \text{ M}$ ). The bond formation between biotin and neutravidin is very rapid, and once formed, it is independent of pH, temperature, organic solvents, and other denaturing agents. Therefore, we used the chemistry between biotin and neutravidin as an effective mechanism for the detection of various protease activities. First, we conjugated neutravidin to the nanoparticles (IONPs-N) by forming an amide bond between the carboxyl groups on the surface of the IONPs and amine groups on the backbone structure of neutravidin (Figure 2A). The hydrodynamic sizes of IONPs and IONPs-N were 60 and 80 nm, as determined by DLS measurements (Figure 2B). The superparamagnetic properties of IONPs and IONPs-N were consistent after neutravidin conjugation, as confirmed by VSM ( $m-H$ ) measurements (Figure S1. B). Also, MPS measurements showed no change in intensity ( $\sim 13 \text{ mV}$ ) and fwhm ( $10 \text{ mT}\mu_0^{-1}$ ) of  $dm(H)/dH$ , plotted as a function of field, further confirming that IONPs remained individually dispersed (no agglomeration) and retained their magnetic properties (Figure

2C), with no significant change in their MPS signal before and after neutravidin conjugation. Then, we added specifically designed linker peptides (GK-8 specific for trypsin and GK-9 for MMP-2) to the IONPs-N to develop our magnetic relaxation-based assays for detection of the proteases.

**Peptide-Mediated MPS-Based Protease Assay.** The central sequences of our peptides were designed with specific protease cleavage sites, flanked with two biotin at both ends (N- and C- terminals). These peptides had a very high adsorption affinity to the surface of the neutravidin conjugated IONPs (IONPs-N). Therefore, IONPs were aggregated immediately after addition of these peptides. We combined this nanoparticle aggregation affinity and protease-induced cleavage of the linker peptides for development of our protease detection assay. This technique enabled us to measure the protease activities, using the magnetic response of the IONPs-N after addition of the peptides. As described in Figure 1, these linker peptides (specifically chosen as substrates for trypsin or MMP-2 proteases) can be cleaved into fragments in the presence of these proteases, resulting in redispersion of the aggregated nanoparticles. This aggregation and redispersion phenomena change the ac magnetization response of the

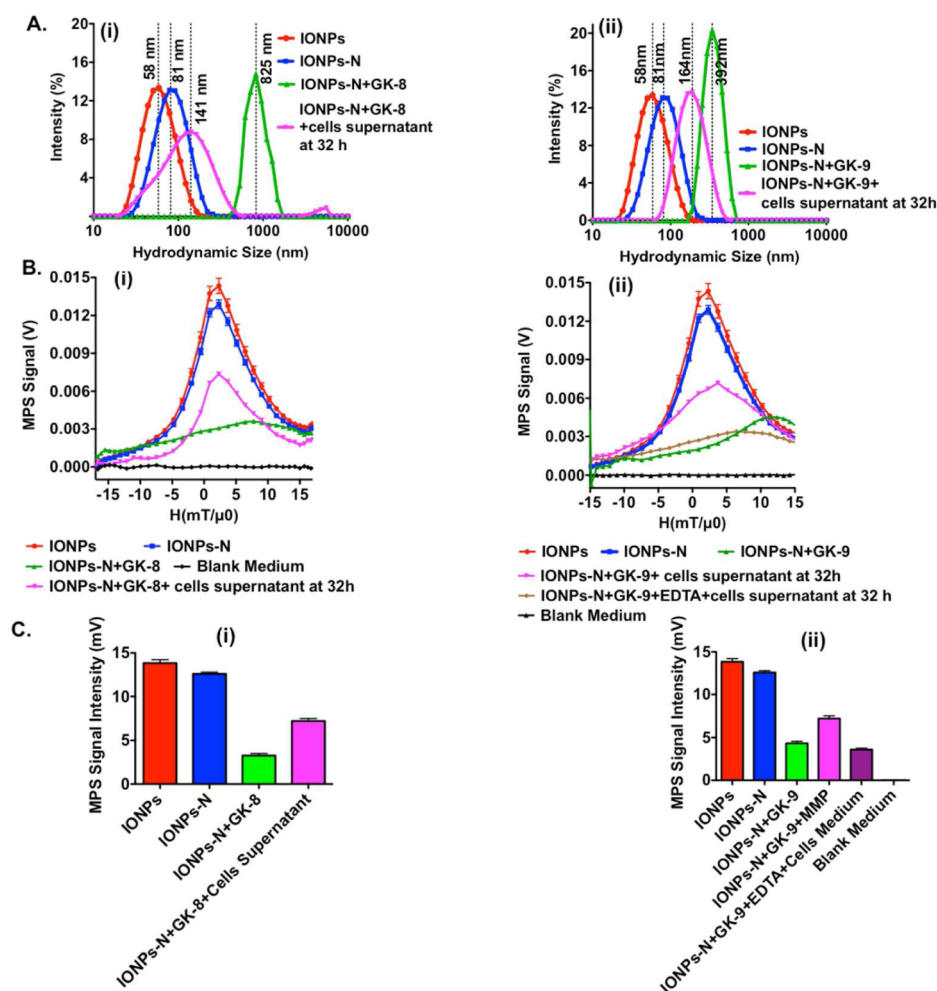


**Figure 5.** In vitro magnetic assay to monitor Trypsin and MMP-2 protease activity in pancreatic carcinoma and HT1080 fibrosarcoma cells. Cells were grown to full confluence, and serum free medium was added to enhance expression of the proteases. IONPs-N-GK-8 and IONPs-N-GK-9 preaggregated complexes were added to the cells supernatant and incubated for 32 h separately. The specific protease secreted from the cells cleaved the targeted linker peptides and effectively redispersed the nanoparticles, a phenomenon clearly detectable qualitatively by our DLS and quantitatively by MPS measurements. (A) DLS results clearly show that the nanoparticles aggregates (IONPs-N+GK-8, ~825 nm and IONPs-N-GK-9, ~392 nm) were redispersed after 32h incubation with cells supernatant, resulting in their smaller hydrodynamic size (IONPs-N+GK-8/GK-9+ cells supernatant, ~141 nm and ~164 nm); MPS results shown in (B) and (C) match with our observations presented and discussed in Figures 3 and 4. The fwhm of the MPS peak (maximum  $dm/dH$ ) was decreased, its peak position shifted to lower field values and signal intensity (peak height) was increased, when aggregated nanoparticles were redispersed in the presence of secreted protease.

nanoparticles (i.e.,  $dm/dH$ ) significantly and can be readily measured by the MPS system (Figures 2C, 3C, and 4C).

Here, we focus on two specific proteases, trypsin and MMP-2, that are expressed during carcinoma, as representative examples of the two different classes of proteases, to illustrate the power of the detection assay. To test for trypsin, a digestive serine protease with a potential role in cancer progression and metastasis,<sup>48</sup> we used an eight amino acid long GK-8 linker peptide as a substrate for trypsin and labeled it with biotin at both N- and C-terminals (Biotin- GPARLAI-K-Biotin) that allowed the interaction with IONPs-N; note that the subsequent cleavage site is indicated in bold. We also developed the assay for MMP-2, which plays a major role in tissue remodeling and degradation of extracellular matrix (ECM).<sup>12</sup> MMPs are expressed by various tissues and pro-inflammatory cells such as endothelial cells, neutrophils, osteoblasts, macrophages, fibroblasts, and lymphocytes.<sup>49</sup> The MMP-2 sensitive linker peptide (GK-9) was nonamer with the sequence Biotin-GGPLGVRGK-Biotin. Mass spectrometry (MS) and high-

performance liquid chromatography (HPLC) analyses showed that molecular weights of the GK-8 and GK-9 peptides were 1293.04 and 1277.70 Da with a purity of up to 99% (data not shown).

Addition of peptides (either GK-8 and GK-9) to IONPs-N causes immediate aggregation of the nanoparticles, leads to the formation of a cloudy colloidal solution, and an increase in hydrodynamic size to 1106.0 and 396.0 nm (Figures 3A and 4A). The VSM data ( $m-H$  curves) showed slightly open loops, formed after addition of the peptides, indicating a ferromagnetic behavior due to aggregation of the nanoparticles (Figures 3B and 4B). The MPS data,  $dm(H)/dH$ , showed the clearest indication of particle binding and agglomeration after addition of GK-8 and GK-9, with FWHMs increasing to 20 and 30  $mT\mu_0^{-1}$  (Figures 3C-i and 4B-i) from 10  $mT\mu_0^{-1}$ , and peak heights decreasing to 5 and 3 mV (Figures 3C-ii and 4C-ii) from 13 mV. These changes in  $dm(H)/dH$  are consistent with our previous reports that presence of aggregates decreases the MPS signal intensity and increases the fwhm of the  $dm(H)/dH$

peaks, since the magnetic response of the aggregates resembles those of nanoparticles with larger core sizes.<sup>39,42,43</sup> Addition of trypsin and MMP-2 proteases to the aggregated IONPs complexes cleaved the specific linker peptides, redispersing the aggregated IONPs, and decreasing the hydrodynamic sizes to 122.4 and 141 nm (Figures 3A and 4A). Magnetically, the redispersed nanoparticles return to superparamagnetic behavior, closing the open hysteresis loops in VSM measurements (Figures 3B-iii and 4B-iii), decreasing the FWHMs to 14 and 18  $\text{mT}\mu_0^{-1}$  (Figures 3C-i and 4C-i) and increasing MPS signal intensities to 12 and 10 mV (Figures 3C-ii and 4C-ii). These data also show that the peptides (GK-8 and GK-9) retained their native conformation for proteolytic recognition and cleavage, even after their interaction with IONPs-N.

**In Vitro Detection of Proteases in Cancer Models.** We also evaluated the in vitro efficacy of this technique for detection of proteases secreted from two representative cancer cell lines (i.e., pancreatic carcinoma for trypsin and fibrosarcoma cells for MMP-2). Cells were cultured in a serum free medium to enhance the expression of proteases. The cell media were collected and incubated with the corresponding preaggregated nanoparticles-peptides complexes. Similar to our previous results, proteases secreted by these cells cleaved the linker peptides and redispersed the IONPs-N, as confirmed by DLS and MPS measurements (Figure 5A(i and ii) and B(i and ii)). We measured the same changes after incubating aggregated nanoparticles (IONPs-N-GK8) with trypsin secreted from human pancreatic carcinoma cell. Trypsin redispersed the nanoparticles, decreased the hydrodynamic size to  $\sim 141$  nm, decreased fwhm, and shifted  $dm/dH$  peak position from 7.7 to 2.3  $\text{mT}\mu_0^{-1}$  and increased MPS signal intensity by a factor of 2, (Figure 5A-i, B-i and C-i). MMP protease expressed by fibrosarcoma cells decreased the hydrodynamic size from 392 to 164 nm (Figure 5A-ii). Also, the position of the  $dm/dH$  peak shifted from 12 to 4  $\text{mT}\mu_0^{-1}$ , decreased fwhm from 30 to and 16  $\text{mT}\mu_0^{-1}$ , (Figure 5B-ii) and increased MPS signal intensity from 4.4 to 7.0 mV (Figure 5C-ii), further confirming the efficacy of the assay.

We developed this technique based on the high binding affinity of neutravidin functionalized nanoparticles (IONPs-N) to specifically designed biotin-peptide linker molecules. The MPS signal did not show any change in the signal intensity after neutravidin conjugation, indicating that the magnetic properties of IONPs did not alter after loading of neutravidin. However, addition of biotin-derived peptides to IONPs-N solution immediately aggregated the nanoparticles. Our results showed that these aggregates can be used as smart and responsive complexes that get cleaved and redispersed in the presence of their target proteases. These two phenomena were clearly discernible by changes in their magnetic response, as shown by the highly sensitive and reproducible changes in the MPS ( $dm/dH$ ) signal. In addition, we have shown before that MPS signal is quantitative and linear with the concentration of IONPs in solutions, down to very low concentrations (i.e. 10  $\mu\text{g}$  Fe/mL).<sup>42</sup> Therefore, these results indicate that simple magnetic relaxation measurement of IONPs, functionalized with specific linker peptides, can be used to detect proteases, quantitatively, in various biological environments including a tumor micro-environment. The procedure described here can be generalized to develop feasible and quick MPS-based assays for detection of proteases avoiding challenges, such as quenching phenomenon or radiation hazards, commonly seen in fluorescence- or radioactive-based techniques.

We have shown that changes in magnetic relaxation of monodisperse nanoparticles, appropriately functionalized with specific linker peptides containing well-defined cleavage sites, can be used as an effective tool for detecting proteases involved in cancer proliferation and metastasis in biological environments. By demonstrating this robust assay for trypsin and MMP-2, representative of the two broad classes of proteases, we provide convincing evidence that this technique can be generalized as a multiplex assay to detect various types of proteases, by selecting and functionalizing the IONPs with their specifically responsive linker peptides or cleavable substrates (e.g., oligonucleotides, lipids, and glycans). This protease detection technique, based on the nanoscale properties of IONPs, can be used to distinguish malignant phenotypes of solid tumors and could be extended for the detection of other hydrolytic enzymes such as lipases, polysaccharides, and nucleases. The science underlying this assay is also a promising route to develop an array of assay conditions (e.g., temperatures, high turbidity, and extreme pH). Such work is also in progress.

## ■ ASSOCIATED CONTENT

### 📄 Supporting Information

The Supporting Information is available free of charge on the ACS Publications website at DOI: 10.1021/acs.nanolett.6b00867.

Experimental information about synthesis, phase transfer, and conjugation of neutravidin to iron oxide nanoparticles, physicochemical characterization of the nanoparticles, synthesis of protease responsive peptides, and synthesis and evaluation of nanoparticle-peptide complexes for detection of the proteases in cancer cell lines (PDF)

## ■ AUTHOR INFORMATION

### Corresponding Author

\*Postal address: Materials Science and Engineering Department, University of Washington, Box 352120, Seattle, WA 98195-2120, USA. Fax number: 206-543-3100. Phone number: 206-543-2814. E-mail address: kannanmk@uw.edu.

### Present Address

S.G.: Amity Institute of Biotechnology, Amity University, Noida, India.

### Notes

The authors declare no competing financial interest.

## ■ ACKNOWLEDGMENTS

The authors are grateful to the National Institutes of Health for support of this research through Grant NIH1R41EB013520-01, 2R42EB013520-02A1, and 1R01EB013689-01/NIBIB.

## ■ REFERENCES

- (1) Crawford, H. C.; Matrisian, L. M. *Inv. Metasta.* **1994**, *14*, 234–245.
- (2) Brik, A.; Wong, C.-H. *Org. Biomol. Chem.* **2003**, *1*, 5–14.
- (3) Noone, P. G.; Zhou, Z.; Silverman, L. M.; Jowell, P. S.; Knowles, M. R.; Cohn, J. A. *Gastroenterology* **2001**, *121*, 1310–1319.
- (4) Bindal, A. K.; Hammoud, M.; Shi, W. M.; Wu, S. Z.; Sawaya, R.; Rao, J. S. *J. Neuro-Oncol.* **1994**, *22*, 101–110.
- (5) Overall, C. M.; Kleinfeld, O. *Nat. Rev. Cancer* **2006**, *6*, 227–239.
- (6) Concha, N. O.; Abdel-Meguid, S. S. *Curr. Med. Chem.* **2002**, *9*, 713–726.



- (7) Schwienhorst, A. *Cell. Mol. Life Sci.* **2006**, *63*, 2773–2791.
- (8) Rakashanda, S.; Rana, F.; Rafiq, S.; Masood, A.; Amin, S. *Biotechnol. Mol. Biol. Rev.* **2012**, *7*, 90–101.
- (9) Ohta, T.; Shimizu, K.; Yi, S.; Takamura, H.; Amaya, K.; Kitagawa, H.; Kayahara, M.; Ninomiya, I.; Fushida, S.; Fujimura, T.; Nishimura, G.; Miwa, K. *Int. J. Oncol.* **2003**, *23*, 61–66.
- (10) Rabassa, A. A.; Schwartz, M. R.; Ertan, A. *Dig. Dis. Sci.* **1995**, *40*, 1997–2001.
- (11) Lyon, M. J. *Dermatol. Ther.* **2010**, *23*, 368–374.
- (12) Martignetti, J. A.; Aqeel, A. A.; Sewairi, W. A.; Boumah, C. E.; Kambouris, M.; Mayouf, S. A. *Nat. Genet.* **2001**, *28*, 261–265.
- (13) Giannelli, G.; Falk-Marzillier, J.; Schiraldi, O.; Stetler-Stevenson, W. G.; Quaranta, V. *Science* **1997**, *277*, 225–228.
- (14) Turk, B. E.; Huang, L. L.; Piro, E. T.; Cantley, L. C. *Nat. Biotechnol.* **2001**, *19*, 661–667.
- (15) Lefkowitz, R. B.; Marciniak, J. Y.; Hu, C. M.; Schmid-Schönbein, G. W.; Heller, M. J. *Electrophoresis* **2010**, *31*, 403–410.
- (16) Lefkowitz, R. B.; Schmid-Schönbein, G. W.; Heller, M. J. *Electrophoresis* **2010**, *31*, 2442–2451.
- (17) Steiner, J. M.; Williams, D. A.; Moeller, E. M.; Melgarejo, T. *Am. J. Vet. Res.* **2000**, *61*, 620–623.
- (18) Morisaka, H.; Hata, K.; Mima, J.; Tanigawa, T.; Furuno, M.; Ishizuka, N.; Tanaka, N.; Ueda, M. *Biosci., Biotechnol., Biochem.* **2006**, *70*, 2154–2159.
- (19) Weeks, I. *Wilson and Wilsons Comprehensive Analytical Chemistry*; Elsevier Publishing Co.: London, 1992; Vol. 29, pp 1–293.
- (20) Ekins, R.; Chu, F.; Micallef, J. J. *Biolumin. Chemilumin.* **1989**, *4*, 59–78.
- (21) Turk, B. *Nat. Rev. Drug Discovery* **2006**, *5*, 785–799.
- (22) Kricka, L. J.; Carter, T. J. N., Eds. *Clinical and Biochemical Luminescence*; Marcel Dekker: New York, 1982; Vol. 12, pp 153–178.
- (23) Harris, J. L.; Backes, B. J.; Leonetti, F.; Mahrus, S.; Ellman, J. A.; Craik, C. S. *Proc. Natl. Acad. Sci. U. S. A.* **2000**, *97*, 7754–7759.
- (24) Twining, S. S. *Anal. Biochem.* **1984**, *143*, 30–34.
- (25) Jones, L. J.; Upson, R. H.; Haugland, R. P.; Panchuk-Voloshina, N.; Zhou, M.; Haugland, R. P. *Anal. Biochem.* **1997**, *251*, 144–152.
- (26) Irvine, G. B.; Ennis, M.; Williams, C. H. *Anal. Biochem.* **1990**, *185*, 304–307.
- (27) Matayoshi, E. D.; Wang, G. T.; Krafft, G. A.; Erickson, J. *Science* **1990**, *247*, 954–958.
- (28) Zhao, M.; Josephson, L.; Tang, Y.; Weissleder, R. *Angew. Chem., Int. Ed.* **2003**, *42*, 1375–1378.
- (29) Holskin, B. P.; Bukhtiyarova, M.; Dunn, B. M.; Baur, P.; de Chastonay, J.; Pennington, M. W. *Anal. Biochem.* **1995**, *227*, 148–155.
- (30) Arami, H.; Khandhar, A.; Liggitt, D.; Krishnan, K. M. *Chem. Soc. Rev.* **2015**, *44*, 8576–8607.
- (31) Arami, H.; Stephen, Z.; Veisoh, O.; Zhang, M. *Adv. Polym. Sci.* **2011**, *243*, 163–184.
- (32) Krishnan, K. M. *IEEE Trans. Magn.* **2010**, *46*, 2523–2558.
- (33) Arruebo, M.; Fernandez-Pacheco, R.; Ibarra, M. R.; Santamaria, J. *Nano Today* **2007**, *2*, 22–32.
- (34) Tomitaka, A.; Ueda, K.; Yamada, T.; Takemura, Y. *J. Magn. Magn. Mater.* **2012**, *324*, 3437–3442.
- (35) Arami, H.; Khandhar, A. P.; Tomitaka, A.; Yu, E.; Goodwill, P. W.; Conolly, S. M.; Krishnan, K. M. *Biomaterials* **2015**, *52*, 251–261.
- (36) Ferguson, R. M.; Khandhar, A. P.; Kemp, S. J.; Arami, H.; Saritas, E. U.; Croft, L. R.; Konkle, J.; Goodwill, P. W.; Halkola, A.; Rahmer, J.; Borgert, J.; Conolly, S. M.; Krishnan, K. M. *IEEE Trans. Med. Imaging* **2015**, *34*, 1077–1084.
- (37) Kalele, S.; Narain, R.; Krishnan, K. M. *J. Magn. Magn. Mater.* **2009**, *321*, 1377–1380.
- (38) Ferguson, R. M.; Minard, K. R.; Khandhar, A. P.; Krishnan, K. M. *Med. Phys.* **2011**, *38*, 1619–1626.
- (39) Ferguson, R. M.; Khandhar, A. P.; Arami, H.; Hua, L.; Hovorka, O.; Krishnan, K. M. *Biomed. Tech.* **2013**, *58*, 493–507.
- (40) Gleich, B.; Weizenecker, J. *Nature* **2005**, *435*, 1214–1217.
- (41) Goodwill, P. W.; Saritas, E. U.; Croft, L. R.; Kim, T.; Krishnan, K. M.; Conolly, S. *Adv. Mater.* **2012**, *24*, 3870–3877.
- (42) Arami, H.; Ferguson, R. M.; Khandhar, A. P.; Krishnan, K. M. *Med. Phys.* **2013**, *40*, 071904.
- (43) Arami, H.; Krishnan, K. M. *J. Appl. Phys.* **2014**, *115*, 17B306.
- (44) Hufschmid, R.; Arami, H.; Ferguson, R. M.; Gonzales, M.; Teeman, E.; Brush, L. N.; Browning, N. D.; Krishnan, K. M. *Nanoscale* **2015**, *7*, 11142–11154.
- (45) Chantrell, R.; Popplewell, J.; Charles, S. *IEEE Trans. Magn.* **1978**, *14*, 975–977.
- (46) Yu, W. W.; Falkner, J. C.; Yavuz, C. T.; Colvin, V. L. *Chem. Commun.* **2004**, *21*, 2306–2307.
- (47) Tomitaka, A.; Arami, H.; Gandhi, S.; Krishnan, K. M. *Nanoscale* **2015**, *7*, 16890–16898.
- (48) Trexler, M.; Briknarová, K.; Gehrmann, M.; Llinás, M.; Patthy, L. *J. Biol. Chem.* **2003**, *278*, 12241–1246.
- (49) Verma, R. P.; Hansch, C. *Bioorg. Med. Chem.* **2007**, *15*, 2223–2268.